# Amplifying organic semiconductor waveguide based nanocrystal sensor

M. Jankauskas, B. Guilhabert, M. D. Dawson and N. Laurand
Institute of Photonics, SUPA Department of Physics, University of Strathclyde, Glasgow, United Kingdom

***Abstract*—** We demonstrate an optical sensor that consists of an amplifying organic semiconductor waveguide with a protective polymer cladding for photostability. Sensing is achieved by evanescence of the guided amplified spontaneous emission (ASE) combining high signal levels at detection with simplicity of implementation. We show correlations between the presence and concentration of colloidal semiconductor nanoparticles on the cladding surface and changes in both the ASE threshold and the optical gain.

## I. INTRODUCTION

Solution-processed organic semiconductors are attractive materials for chemical and biological sensing using stimulated emission [1-3]. However, they are also susceptible to photochemical damage in ambient atmosphere, especially at the pumping intensities required to operate in the stimulated emission regime. Here, we report a sensor that addresses this issue by physically separating the organic semiconductor from the sensing region while still enabling optical interactions, hence sensing, by evanescence. The device is based on an amplifying waveguide structure and has the potential to match or even exceed the sensitivity of standard waveguide sensors. It is also extremely simple to fabricate and to implement. In the following, we describe the design and concept of the sensor as well as its fabrication. We then demonstrate the detection of colloidal semiconductor nanoparticles present in different concentrations on the device surface.

## II. DESIGN, MATERIALS, FABRICATION AND MEASUREMENTS METHOD

### *A. Design and Materials*

The structure of the amplifying waveguide is shown schematically in the inset of Fig. 1. It is made of a glass substrate, a 130 nm thick organic semiconductor layer (the core of the waveguide structure that can amplify the light) and a 180 nm polymer cladding, which also acts as an encapsulant. For sensing, the waveguide is optically-pumped above the amplified spontaneous emission (ASE) threshold. In this regime, ASE is coupled into the guided mode whose emission is simply detected with no added optics as explained in section II.C. The evanescent tail of the guided mode extends through the cladding and optically probes the device's surface. Nanoparticles/analytes adsorbed onto this surface change the complex refractive index and in turn affect the properties of the guided mode, including the optical gain, intensity and ASE threshold. These parameters can be monitored for detection.

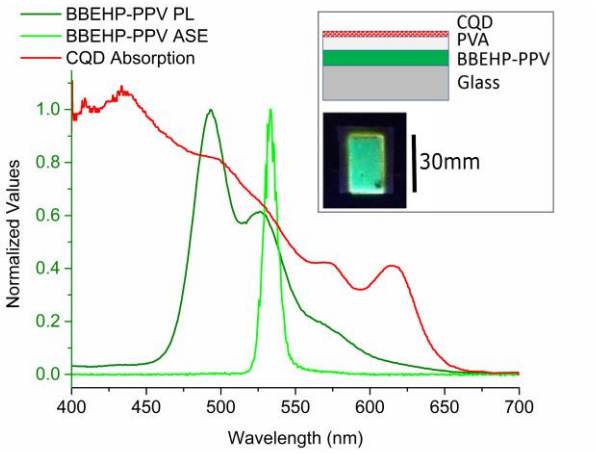


Fig. 1. Emission spectra of BBEHP-PPV and absorption spectra for Colloidal Quantum Dots (CQD). Inset: (top) schematized waveguide; (bottom) photo of a sample under UV

The core of the amplifying waveguide is made of a conjugated polymer, BBEHP-PPV [2,3]. BBEHP-PPV has been shown to combine low threshold for stimulated emission with relatively high photostability [1-3]. Fig. 1 displays the typical photoluminescence (PL) and ASE spectra of a BBEHP-PPV thin film. The PL maximum is at a 500 nm wavelength with a secondary excitonic peak at 530 nm. The ASE, characterized by its narrower spectrum (<5nm), is centered at ~535 nm.

Poly (vinyl alcohol) $(C_2H4O)_n$ (molecular weight of 85,000 – 124,000), abbreviated as PVA, is used for the cladding. PVA is transparent in the visible and has low oxygen permeability. It has been shown that even a very thin film of PVA increases the photodegradation dosage of BBEHP-PPV [4]. In addition, PVA is water soluble, while BBEHP-PPV is not, which facilitates the fabrication.

Core/shell CdSeS/ZnS colloidal quantum dots (CQD) are used here as analytes (inset of Fig.1). These have a nominal diameter of 6 nm, luminesce at 630 nm and their absorption spectrum overlaps the ASE wavelength of BBEHP-PPV (Fig. 1). Different concentrations of CQDs are deposited on the waveguide surface for the sensor proof of concept.

### *B. Fabrication*

The waveguide structure is fabricated entirely by spin coating under ambient atmosphere. The 130 nm BBEHP-PPV layer is formed onto the glass substrate by spin-coating a solution of 20 g/l BBEHP-PPV in toluene at 5000 revolutions per minute (RPM) for 60 s. Next the ~180 nm PVA layer is

deposited from a 50 g/l PVA/deionized water solution spun at 3200 RPM for 60 s. The samples are subsequently left to dry on a hotplate at 35ºC for ~3 days. CQD solutions are prepared at various concentrations (10-100 g/l) with the solvent being a 50%/50% mix of chloroform and toluene. Poly(methyl methacrylate) is also added to the mix at 1.6 g/l. CQD solutions are then spin coated onto the samples at 3000 RPM. At the highest concentration, the CQD form a close-packed film of ~300-500 nm in thickness [5]. Lower concentrations lead to thinner and sparser films.

### *C. Measurement Method*

A 355 nm laser (5 ns pulses) shaped into a 100 μm wide stripe beam, with homogenous fluence along its length, is used to pump the sample through the substrate at normal incidence. The excitation length $l$ can be varied between 500 and 3000 μm. The edge emission of the stripe-excited sample is directly collected by a 50 μm core fiber coupled into a CCD spectrometer for analysis.

The ASE threshold for a given $l$ is defined as the pump fluence above which the spontaneous emission guided in the device is significantly amplified, predominantly around the maximum of the spectral gain, resulting in a narrowing of the edge emission spectrum. When pumping above the ASE threshold, the edge emission intensity $I(l)$ increases exponentially with the stripe length $l$ (1). This enables the evaluation of the modal gain, $g$, using the variable stripe length (VSL) method, fitting (1) to the data [6]. In (1) $A_0$ is a parameter related to the emission cross section and the pump energy.

$$I(l) = \frac{A_0[\exp(gl)-1]}{g} \quad (1)$$

To demonstrate proof-of-principle sensing using our device, the modal gain $g$ and the ASE threshold are measured on samples with different CQD concentrations. A sample with no CQDs deposited is called the 'neat sample' and is used as a reference. Other samples are referred to by the CQD solution concentration utilized at fabrication.

## III. RESULTS

### *D. Microscope images*

Fig. 2 shows optical micrographs of the surface of the samples under microscope with a 100x magnification. The black rectangle boxes are parts of the images that were post-processed and colorized (red) to increase the visibility of quantum dot structures on top of the samples. Samples in Fig. 2 b-d can be clearly seen to have an increasing amount of CQDs

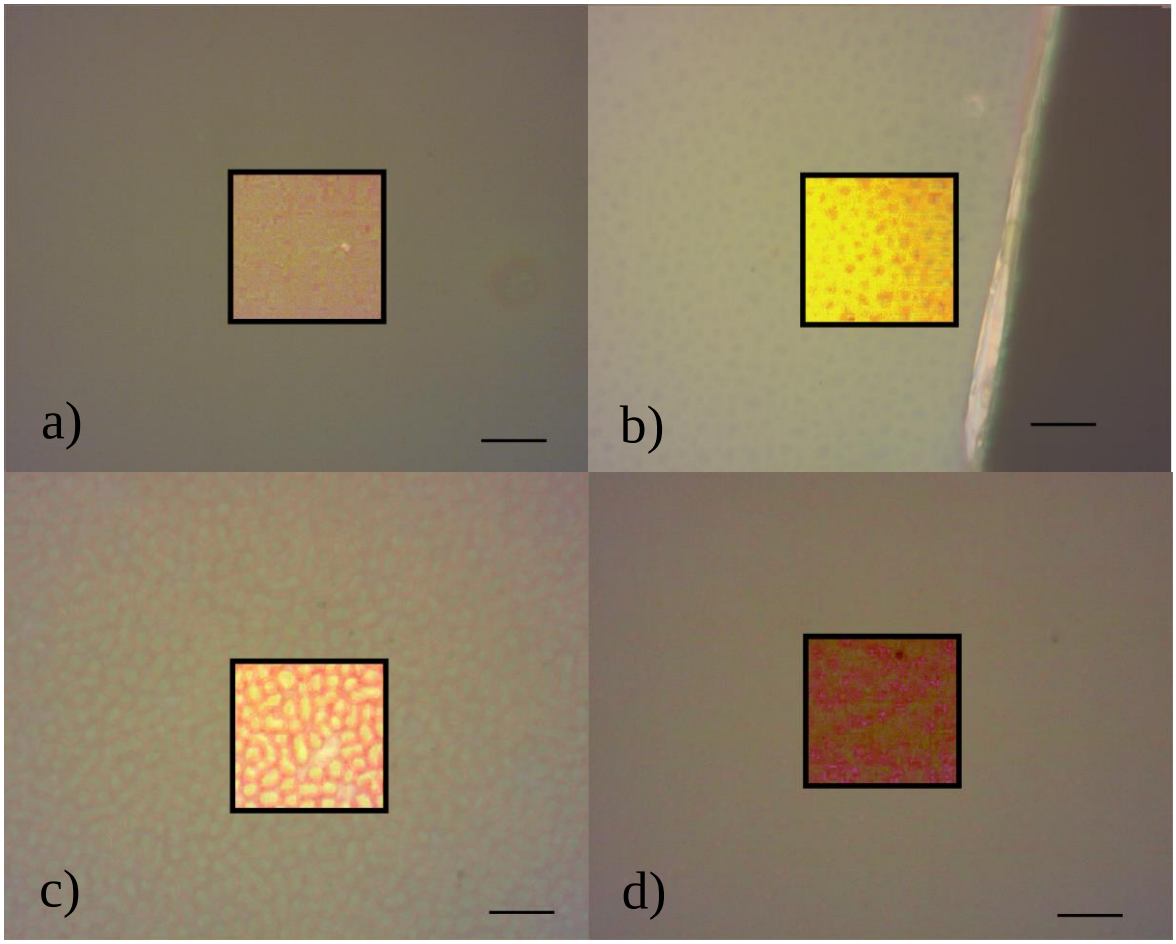


Fig. 2. Microscope images under 100x magnification of the surface of samples coated with **a)** 5g/l, **b)** 10g/l, **c)** 20g/l, and **d)** 100g/l CQD solutions. The scale bar is 10μm. The rectangular insets show a part of the images that was post-processed and colorized to increase the contrast..

and the layers are not completely homogenous at small concentration. However, the scale of the patterns, 2-5 μm, is much smaller compared to the stripe width of ~100 μm and the step of the variable stripe length used in the experiments (~45 μm).

### *E. Threshold*

Fig. 3 shows the evolution of the intensity for different samples as the pump fluence is increased while the stripe length is fixed at 635 μm. The ASE threshold increases with the CQD concentration from ~50 μJ/cm$^2$ for the neat sample, up to ~120 μJ/cm$^2$ and >400 μJ/cm$^2$ for the samples prepared with 20 g/l and 100 g/l, respectively. A higher concentration of CQD solution (see section II) leads to more CQDs on the surface and therefore a higher absorption for the guided mode. For small concentration (<5 g/l) the threshold is found to be close to that of the neat sample given the measurement parameters.

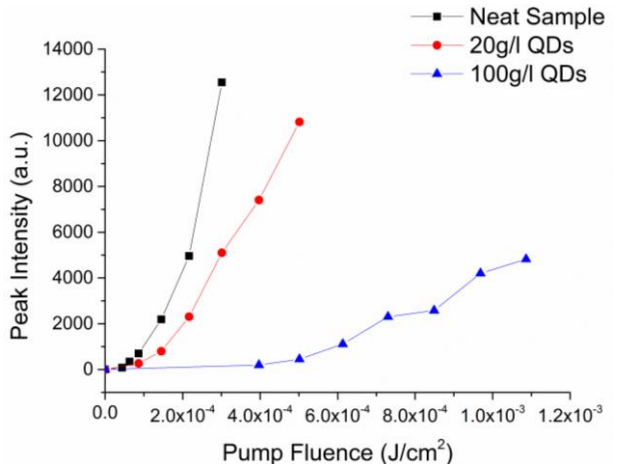


Fig. 3. ASE intensity versus pump fluence for samples with different concentrations of CQDs.

### *F. Variable Stripe Length measurements*

Fig. 4 shows the evolution of the intensity as the pump stripe length is increased. All samples are measured at a 216 μJ/cm$^2$ pump fluence. Fitting the data with (1) gives modal gain values (standard error in brackets) of 36 cm$^{-1}$(+/-2.3), 40 cm$^{-1}$(+/-3.0), 9 cm$^{-1}$(+/-0.7) and 5 cm$^{-1}$(+/-0.2) for the neat, 5 g/l CQD, 10 g/l CQD and 20 g/l CQD samples, respectively. This shows that the decrease in gain when CQDs are present on the device surface scales with the amount of CQDs. The gain values for neat and 5g/l samples fall within the error from each other.

## IV. Conclusion

An amplifying organic semiconductor waveguide sensor incorporating a protective cladding for enhanced photostability and analyte separation has been demonstrated. Comparing a device with no CQDs on its surface to one prepared with a CQD solution of 20 g/l (estimated to form 60 nm film), the optical gain drops from 36 cm$^{-1}$ down to 5 cm$^{-1}$ while at the same time the ASE threshold increases from ~50 μJ/cm$^2$ to ~120 μJ/cm$^2$. Reducing the concentration of CQDs on the surface we observe smaller differences in the threshold of ASE. However, the decrease in optical gain is still significant and experiments are under way to determine the detection limit of the device.

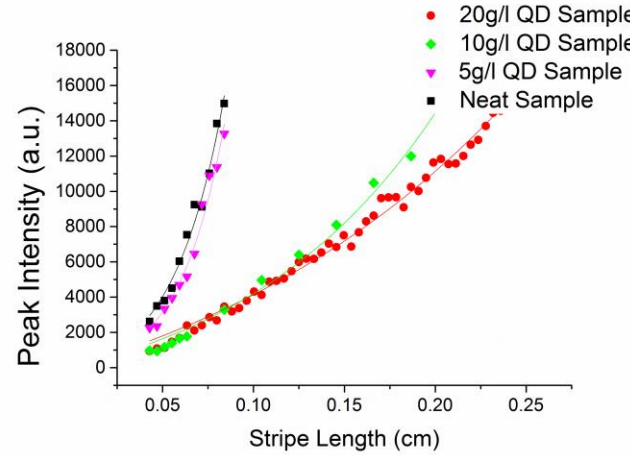


Fig. 4. VSL measurement data. Solid lines are fits. Gain values are 36 cm$^{-1}$(Neat), 40cm$^{-1}$(5g/l), 9 cm$^{-1}$(10g/l) and 5 cm$^{-1}$(20g/l).


## Acknowledgment

The authors would like to thank A. L. Kanibolotsky and P. J. Skabara for synthesis of the BBEHP-PPV.


## Supporting Information

The raw data from the measurement experiments can be found at: http://dx.doi.org/10.15129/7fb0d98d-1f2d-4a24-a864-2df84708404f

## References


[1] Y. Yang, G. Turnbull and I. Samuel, "Sensitive Explosive Vapor Detection with Polyfluorene Lasers", Advanced Functional Materials, vol. 20, no. 13, pp. 2093-2097, 2010.

[2] A. Rose, Z. Zhu, C. Madigan, T. Swager and V. Bulović, "Sensitivity gains in chemosensing by lasing action in organic polymers", Nature, vol. 434, no. 7035, pp. 876-879, 2005.

[3] A. Haughey, G. McConnell, B. Guilhabert, G. Burley, M. Dawson and N. Laurand, "Organic Semiconductor Laser Biosensor: Design and Performance Discussion", IEEE Journal of Selected Topics in Quantum Electronics, vol. 22, no. 1, pp. 6-14, 2016.

[4] C. Foucher, B. Guilhabert, A. Kanibolotsky, P. Skabara, N. Laurand and M. Dawson, "Highly-photostable and mechanically flexible all-organic semiconductor lasers", Optical Materials Express, vol. 3, no. 5, p. 584, 2013.

[5] L. McLellan, B. Guilhabert, N. Laurand and M. Dawson, "CdS_xSe_1-x/ZnS semiconductor nanocrystal laser with sub 10kW/cm^2 threshold and 40nJ emission output at 600 nm", Optics Express, vol. 24, no. 2, p. A146, 2015.

[6] K. Shaklee, R. Nahory and R. Leheny, "Optical gain in semiconductors", Journal of Luminescence, vol. 7, pp. 284-309, 1973.